

## Synthesis, Properties and Environmentally Important Nanostructured and Antimicrobial Supramolecular Coordination Polymers Containing 5-(3-Pyridyl)-1,3,4-Oxadiazole-2-Thiol and Benzimidazole

Aref AM Aly\*, Mahmoud A Ghandour, Bahaa M Abu-Zied and Maged S Al-Fakeh

Department of Chemistry, Faculty of Science, Assiut University, Assiut Egypt

### Abstract

A new series of coordination polymers of Co(II), Ni(II), Cu(II), Cd(II) and UO<sub>2</sub>(II), 5-(3-pyridyl)-1,3,4-oxadiazole-2-thiol (POZT) and benzimidazole (BIMZ) has been prepared and characterized. The compounds have been characterized based on elemental analysis, FT-IR and electronic spectral studies, thermal analysis and X-ray powder diffraction. Thermogravimetry (TG), derivative thermogravimetry (DTG) and differential thermal analysis (DTA) have been used to study the thermal decomposition steps and to calculate the thermodynamic parameters of the nano-sized metal coordination polymers. The kinetic parameters have been calculated making use of the Coats-Redfern and Horowitz-Metzger equations. The scanning electron microscope SEM photographs and particle size calculations from the powder XRD data indicate the nano-sized nature of the prepared supramolecular coordination polymers (average size 17-28 nm). The antimicrobial activity of the synthesized compounds was tested against six fungal and five bacterial strains. The majority of compounds were effective against the tested microbes. The bacteria and fungi strains are common contaminants of the environment in Egypt. In this article the studied strains are frequently reported from contaminated soil, water and food.

**Keywords:** Coordination polymers; X-ray powder diffraction, Thermal studies and biological activity.

### Introduction

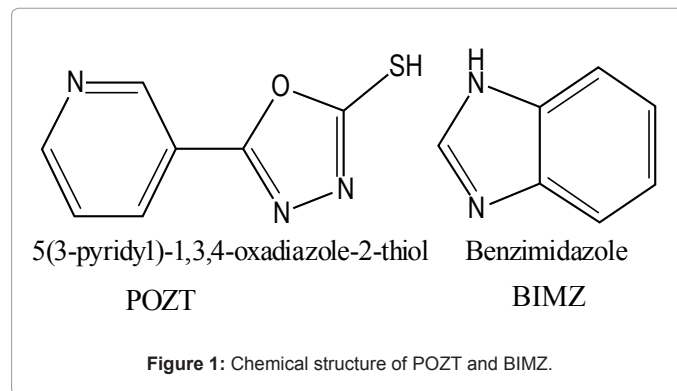
In recent decades, metal-organic frameworks (MOFs) are extensively developed as a new type of functional crystalline materials for a wide range of promising applications in separation, storage, exchange, and heterogeneous catalysis due to their high stability and structural diversity [1-4]. In general, the final coordination polymers significantly depend on the metal and ligand precursors [5]. Recently, a variety of pyridyl connectors have been extensively applied in this facet [6]. It should be noted that organosulfur compounds, which play an important role in chemical or biological processes are well documented [7]. Heterocyclic thiones are known in the field of coordination chemistry because of their potential multifunctional donor sites, viz either exocyclic sulfur or endocyclic nitrogen [8]. The pyridyl oxadiazoles are suitable bridging ligands for the synthesis of coordination polymers and several papers were published on using cyclized pyridyl 1,3,4-oxadiazoles for the preparation of metal complexes [9-11]. By changing the steric and electronic properties of ancillary organic ligands such as the heterocycle N-donor molecules, (e.g. benzimidazole), it was possible to modulate the construction and the dimension of the polymeric coordination network [12]. Also benzimidazole belongs to a class of compounds which are of interest because of their pharmaceutical, analytical, most common binding sites in various metalloenzymes and industrial applications [13]. The chemistry of uranium is the most developed, due to the low radioactivity of one of its isotopes and its wide use at industrial and laboratory scales [14]. Uranium (VI) tends to form linear cation with two oxygen atoms UO<sub>2</sub><sup>2+</sup> which can be further surrounded by a number of anions commonly lying in one plane, which is perpendicular to O-U-O structure [15]. In this work, we synthesized and characterized new coordination polymers derived from the bridging ligand 5-(3-pyridyl)-1,3,4-oxadiazole-2-thiol, benzimidazole and Co(II), Ni(II), Cu(II), Cd(II) and UO<sub>2</sub>(II).

### Material and Methods

High purity 5-(3-pyridyl)-1,3,4-oxadiazole-2-thiole and benzimidazole were supplied from Sigma Aldrich and Merck. All other chemicals were of AR grade. Figure 1 shows the structure of the ligands.

### Physical measurements

Elemental analysis (carbon, hydrogen, nitrogen and sulphur) were



\*Corresponding author: Aref A.M. Aly, Department of Chemistry, Faculty of Science, Assiut University, Assiut Egypt, Tel: +201003486619; Fax: 0020-88-2342708; E-mail: [aref\\_20002001@yahoo.com](mailto:aref_20002001@yahoo.com)

Received February 03, 2012; Accepted February 24, 2012; Published February 26, 2012

Citation: Aly AAM, Ghandour MA, Abu-Zied BM, Al-Fakeh MS (2012) Synthesis, Properties and Environmentally Important Nanostructured and Antimicrobial Supramolecular Coordination Polymers Containing 5-(3-Pyridyl)-1,3,4-Oxadiazole-2-Thiol and Benzimidazole. J Environment Analytic Toxicol 2:129. doi:10.4172/2161-0525.1000129

Copyright: © 2012 Aly AAM, et al. This is an open-access article distributed under the terms of the Creative Commons Attribution License, which permits unrestricted use, distribution, and reproduction in any medium, provided the original author and source are credited.

performed using Analytischer Funktionstest Vario El Fab-Nr.11982027 elemental analyzer. Infrared spectra were recorded as KBr disks ( $400\text{--}4000\text{ cm}^{-1}$ ) with a FT-IR spectrophotometer model (Thermo-Nicolet-6700 FTIR) and the electronic spectra were obtained using a Shimadzu UV-2101 PC spectrophotometer. Magnetic susceptibility measurements were done on a magnetic susceptibility balance of the type MSB-Auto. The conductance was measured using a conductivity Meter model 4310 JENWAY. Thermal studies were carried out in dynamic air on a Shimadzu DTG 60-H thermal analyzer at a heating rate  $10^\circ\text{C min}^{-1}$ . XRD Model PW 1710 control unit Philips, Anode material Cu 40 K.V 30 M.A Optics: Automatic divergence slit. Scanning electron microscope (JEOL JFC-1100E ION SPUTTERING DEVICE, JEOL JSM-5400LV SEM), SEM specimens were coated with gold to increase the conductivity. For the biological activity all microbial strains were kindly provided by the Assiut University Mycological Centre (AUMC), Egypt. These strains are common contaminants of the environment in Egypt and some of which are involved in human and animal diseases (*Candida albicans*, *Geotrichum candidum*, *Scopulariopsis brevicaulis*, *Aspergillus flavus*, *Staphylococcus aureus*), plant diseases (*Fusarium oxysporum*) or frequently reported from contaminated soil, water and food substances (*Escherichia coli*, *Bacillus cereus*, *Pseudomonas aeruginosa* and *Serratia marcescens*). To prepare inocula for bioassay, bacterial strains were individually cultured for 48h in 100 ml conical flasks containing 30 ml nutrient broth medium. Fungi were grown for 7 days in 100 ml conicals containing 30 ml Sabouraud's dextrose broth. Bioassay was done in 10 cm sterile plastic Petri plates in which microbial suspension (1 ml/plate) and 15 ml appropriate agar medium (15 ml/plate) were poured. Nutrient agar and Sabouraud's dextrose agar were respectively used for bacteria and fungi. After solidification of the media, 5 mm diameter cavities were cut in the solidified agar (4 cavities/plate) using sterile cork borer. The chemical compounds dissolved in dimethyl sulfoxide (DMSO) at 2%w/v (=20 mg/ml) were pipetted in the cavities (20  $\mu\text{l}$  /cavity). Cultures were then incubated at  $28^\circ\text{C}$  for 48 h in case of bacteria and up to 7 days in case of fungi. Results were read as the diameter (in mm) of inhibition zone around cavities [16].

### Synthesis of the coordination polymers

**[Co(POZT)(BIMZ)Cl(H<sub>2</sub>O)<sub>2</sub>]<sub>n</sub> (1):** A methanolic solution (10 mL) of POZT (0.1 g, 0.5 mmol) was slowly added into a hot methanolic solution (10 mL) of CoCl<sub>2</sub>·6H<sub>2</sub>O (0.132 g, 0.5 mmol) and to it a methanolic solution (10 mL) of benzimidazole (0.066 g, 0.5 mmol) was added drop wise. The resultant mixture was stirred for 1 h and filtered. The dark blue precipitate was separated, washed with distilled water and EtOH and then dried over CaCl<sub>2</sub> in a desiccator. Anal. Calc. for CoC<sub>14</sub>H<sub>13</sub>N<sub>5</sub>SO<sub>3</sub>Cl: C, 39.49; H, 3.08; N, 16.45; S, 7.53. Found: C, 39.11; H, 4.76; N, 15.91; S, 6.22. IR data:  $\nu_{\text{OH}}$  3196 (s),  $\nu_{\text{C=N}}$  1608 (s),  $\nu_{\text{C-N}}$  1460 (s), 906 (s),  $\nu_{\text{M-O}}$  552 (m),  $\nu_{\text{M-N}}$  424 (m)  $\text{cm}^{-1}$ , m.p.  $280^\circ\text{C}$ .

**[Ni(POZT)(BIMZ)Cl(H<sub>2</sub>O)<sub>2</sub>].3H<sub>2</sub>O (2):** It was synthesized adopting the same procedure as in case of 1. The molar ratio was 1:1:1, NiCl<sub>2</sub>·6H<sub>2</sub>O (0.132g, 0.5 mmol), POZT (0.1g, 0.5 mmol) and BIMZ (0.066g, 0.5 mmol). A Green compound was isolated. Anal. Calc. for NiC<sub>14</sub>H<sub>19</sub>N<sub>5</sub>SO<sub>3</sub>Cl: C, 35.05; H, 4.00; N, 14.60; S, 6.68. Found: C, 33.47; H, 3.86; N, 14.14; S, 7.99. IR data:  $\nu_{\text{OH}}$  3385 (s), 3150 (w),  $\nu_{\text{C=N}}$  1606 (s),  $\nu_{\text{C-N}}$  1485 (s), 964 (m),  $\nu_{\text{M-O}}$  560 (m),  $\nu_{\text{M-N}}$  432 (m)  $\text{cm}^{-1}$  m.p.  $285^\circ\text{C}$ .

**[Cu(POZT)(BIMZ)Cl(H<sub>2</sub>O)<sub>2</sub>].3H<sub>2</sub>O (3):** A similar synthetic method as that for 1 was used except that the reaction solvent was replaced by ethanol (10 mL). A brown compound was obtained. Anal. Calc. for CuC<sub>14</sub>H<sub>19</sub>N<sub>5</sub>SO<sub>3</sub>Cl: C, 34.70; H, 3.96; N, 14.45; S, 6.62. Found:

C, 33.42; H, 4.37; N, 14.01; S, 7.98. IR data:  $\nu_{\text{OH}}$  3495 (s), 3192 (m),  $\nu_{\text{C=N}}$  1612 (s),  $\nu_{\text{C-N}}$  1466 (s), 906 (s)  $\nu_{\text{M-O}}$  572 (m),  $\nu_{\text{M-N}}$  440 (s)  $\text{cm}^{-1}$ , m.p.  $276^\circ\text{C}$ .

**[Cd(POZT)(BIMZ)Cl(H<sub>2</sub>O)<sub>2</sub>].3H<sub>2</sub>O (4):** The same synthetic procedure as that for 1 was adopted except that CoCl<sub>2</sub>·6H<sub>2</sub>O (0.132 g, 0.5 mmol) was replaced by CdCl<sub>2</sub>·2H<sub>2</sub>O (0.127 g, 0.5 mmol) (Figure 2). A white product was isolated. Anal. Calc. for CdC<sub>14</sub>H<sub>19</sub>N<sub>5</sub>SO<sub>3</sub>Cl: C, 31.52; H, 3.59; N, 13.13; S, 6.01. Found: C, 33.96; H, 4.25; N, 11.72; S, 7.22. IR data:  $\nu_{\text{OH}}$  3500 (s), 3190 (m),  $\nu_{\text{C=N}}$  1620 (s), 1483 (s), 928 (m),  $\nu_{\text{M-O}}$  550 (m),  $\nu_{\text{M-N}}$  430 (m)  $\text{cm}^{-1}$ , m.p.  $298^\circ\text{C}$ .

**[UO<sub>2</sub>(POZT)(BIMZ)(ace)(H<sub>2</sub>O)]<sub>n</sub> (5):** A mixture of equimolar quantity (0.5 mmol) of UO<sub>2</sub>(ac)<sub>2</sub>·2H<sub>2</sub>O (0.236 g) and POZT (0.1 g) in a methanolic solution (15 mL) was mixed with a methanolic solution (10 mL) of BIMZ (0.066 g, 0.5 mmol) and heated for 2 h, then gradually cooled to room temperature (Figure 3). A yellow compound was isolated. Anal. Calc. for UO<sub>2</sub>C<sub>16</sub>H<sub>14</sub>N<sub>5</sub>SO<sub>4</sub>: C, 29.91; H, 2.20; N, 10.90; S, 5.00. Found: C, 30.30; H, 3.71; N, 9.96; S, 6.78. IR data:  $\nu_{\text{OH}}$  3200 (m),  $\nu_{\text{C=N}}$  1618 (s),  $\nu_{\text{C-N}}$  1410 (m), 924 (m),  $\nu_{\text{M-O}}$  520 (m),  $\nu_{\text{M-N}}$  430 (m)  $\text{cm}^{-1}$ , m.p.  $298^\circ\text{C}$ .

### Results

The coordination polymers were prepared by the reaction of 5-(3-pyridyl)-1,3,4-oxadiazole-2-thiol (neutralized with NaOH), metal chlorides or acetate, and benzimidazole (dissolved in EtOH or MeOH). The prepared compounds were found to react in the molar ratio 1: 1: 1 metal: POZT: BIMZ. The complexes are air stable, insoluble in

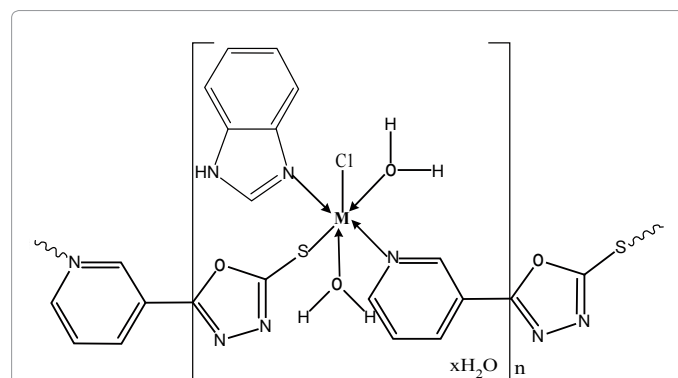


Figure 2: Suggested structure of  $[\text{Cd}(\text{M}(\text{POZT})(\text{BIMZ})\text{Cl}(\text{H}_2\text{O})_2)_n \cdot x\text{H}_2\text{O}]$ , M = Co(II), Ni(II), Cu(II) and Cd(II) x = 0 or 3.

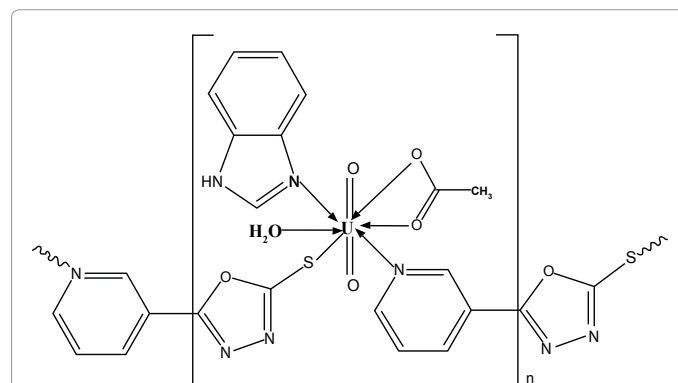


Figure 3: Suggested structure of  $[\text{UO}_2(\text{POZT})(\text{BIMZ})(\text{ace})(\text{H}_2\text{O})]_n$

common organic solvents but partially soluble in DMSO. The electrical conductivity of the coordination polymers adequately supported their non-electrolytic nature.

### Fourier transform infrared spectroscopy (FT-IR)

The main IR bands of each compound are cited in the experimental part. The bands observed in the 1606-1620  $\text{cm}^{-1}$  regions are assigned to the  $\nu(\text{C}=\text{N})$  stretching vibration of the POZT [17]. BIMZ exhibits two bands in the regions 906-964, 1414-1485  $\text{cm}^{-1}$  which can be assigned to  $\nu(\text{C}-\text{N})$  ring [12]. Furthermore, it is found that the bands at 3385-3500  $\text{cm}^{-1}$  in the spectra of compounds 2, 3 and 4 are assigned to  $\nu\text{OH}$  of water of crystallization [18] whereas the  $\nu\text{OH}$  stretching vibrations of the coordinated water molecules are located in the range 3150-3200  $\text{cm}^{-1}$  for all compounds [19]. Metal-oxygen and metal-nitrogen bonding are manifested by the appearance of a band in the 520-572  $\text{cm}^{-1}$  and 424 - 440  $\text{cm}^{-1}$  region, respectively [20].

### Electronic Spectra

The UV-Vis spectra of the coordination polymers in dimethylsulphoxide (DMSO) display two absorption maxima located in the regions 34,482- 39,682 and 21,186 - 27,777  $\text{cm}^{-1}$  which are attributed to  $\pi \rightarrow \pi^*$  and  $n \rightarrow \pi^*$  transitions within the POZT and BIMZ ligands [12,16]. The Co(II), Ni(II) and Cu(II) coordination polymers exhibit a band at 16,129, 17,543 and 15,337  $\text{cm}^{-1}$  respectively corresponding to the d-d transitions. Additionally, the magnetic moments of the compounds were measured and it has been found that the cobalt(II) compound 1 has a magnetic moment of 4.43 B.M typical for the octahedral complexes [21] whereas the magnetic moment values 1.90, 2.10 B.M were found for the Ni(II) 3 and Cu(II) 4 compounds respectively suggesting their octahedral structures [22,23]. However, the low value of magnetic moment for the Ni(II) complex may be attributed to the presence of a mixture of square planar and octahedral geometries [24]. The electronic spectral data are shown in (Table 1). From the above data the structure of the coordination polymers can be postulated as follows:

### Thermal Studies

The thermal decomposition of the coordination polymers has been investigated in dynamic air from ambient temperature to 750°C (Table 2). As a following example the thermogram of the cadmium(II) compound 4 shows four stages in the temperature ranges 53-92, 93-176, 177-235 and 236-750°C (Figure 4). The first and second stages correspond to the release of the two coordinated and the three crystalline water molecules (calc.16.89 %, found 15.32 %). The DTG curve shows these two steps at 63 and 131°C and two endothermic peaks at 66 and 133°C are recorded in the DTA trace. The third and fourth steps represent decomposition of the organic ligands. These two steps are manifested by two DTG peaks at 200 and 525°C and are associated with two exothermic peaks at 201 and 527°C in the DTA curve. The final product was identified on the basis of mass loss considerations to be CdO (calc. 24.07 %, found 25.76 %). (Scheme 1).

**Kinetic analysis:** Non-isothermal kinetic analysis of the complexes was carried out applying two different procedures: the Coats-Redfern [24] and the Horowitz-Metzger [25] methods.

#### (i) The Coats-Redfern equation

$$\ln[1-(1-\alpha)^{1-n}/(1-n)T^2] = M/T + B \text{ for } n \neq 1 \quad (1)$$

$$\ln[-\ln(1-\alpha)/T^2] = M/T + B \text{ for } n = 1 \quad (2)$$

where  $\alpha$  is the fraction of material decomposed,  $n$  is the order of

Compounds	$\nu \text{ max}(\text{cm}^{-1})$	Assignment	$\mu_{\text{eff}}$ B.M
1	16,129	d-d transition	4.43
	25,125	$n \rightarrow \pi^*$ transition	
	35,211	$\pi \rightarrow \pi^*$ transition	
2	17,543	d-d transition	2.10
	27,777	$n \rightarrow \pi^*$ transition	
	35,971	$\pi \rightarrow \pi^*$ transition	
3	15,337	d-d transition	1.90
	21,186	$n \rightarrow \pi^*$ transition	
	34,482	$\pi \rightarrow \pi^*$ transition	
4	27,472	$n \rightarrow \pi^*$ transition	-
	39,682	$\pi \rightarrow \pi^*$ transition	
5	14,752	d-d transition	-
	27,322	$n \rightarrow \pi^*$ transition	
	39,525	$\pi \rightarrow \pi^*$ transition	

Table 1: Electronic spectral data and magnetic moments of the compounds.

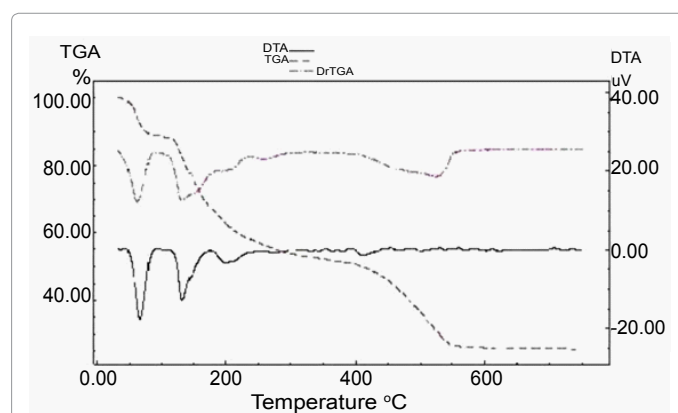


Figure 4: TG, DTG and DTA thermo grams of compound 4 in dynamic air.

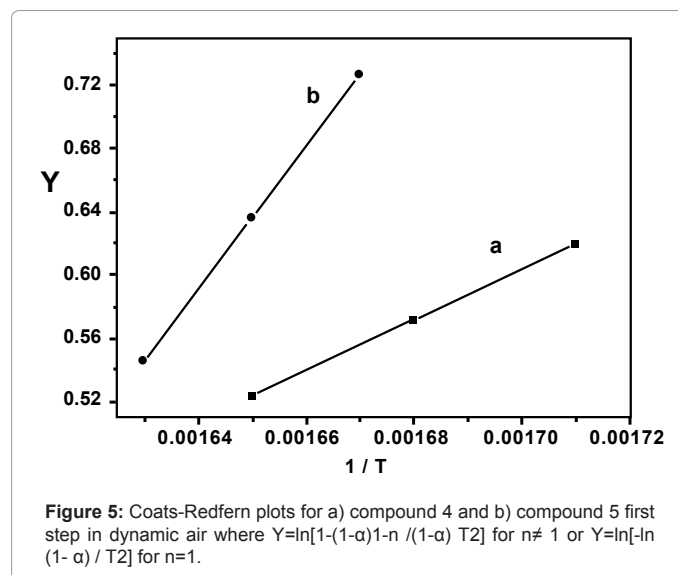


Figure 5: Coats-Redfern plots for a) compound 4 and b) compound 5 first step in dynamic air where  $Y = \ln[1-(1-\alpha)^{1-n}/(1-n)T^2]$  for  $n \neq 1$  or  $Y = \ln[-\ln(1-\alpha)/T^2]$  for  $n=1$ .

the decomposition reaction and  $M = -E/R$  and  $B = ZR/\Phi E$ ;  $E$ ,  $R$ ,  $Z$  and  $\Phi$  are the activation energy, gas constant, pre-exponential factor and heating rate, respectively.

#### (ii) The Horowitz-Metzger equation

$$\ln[1-(1-\alpha)^{1-n}/(1-n)] = \ln ZRT^2/\Phi E - E/RT + E\theta/RT^2 \text{ for } n \neq 1 \quad (3)$$

$$\ln[-\ln(1-\alpha)] = E\theta/RT^2 \text{ for } n = 1 \quad (4)$$

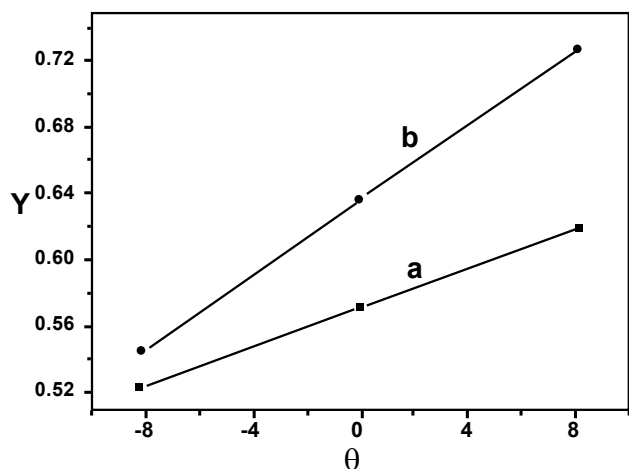


Figure 6: Horowitz-Metzger plots for a) compound 4 and b) compound 5 first step in dynamic air where  $Y = \ln[1 - (1 - \alpha)^{1-n} / (1 - n)]$  for  $n \neq 1$  or  $Y = \ln[-\ln(1 - \alpha)]$  for  $n = 1$ .

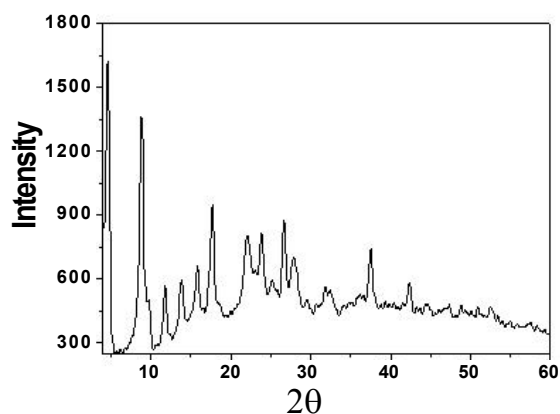


Figure 7: X-ray powder diffraction of  $[[\text{Cu}(\text{POZT})(\text{BIMZ})\text{Cl}(\text{H}_2\text{O})_2] \cdot 3\text{H}_2\text{O}]_n$ .

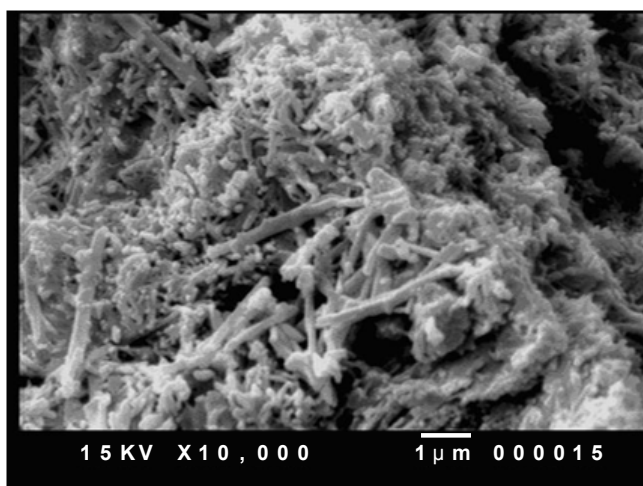


Figure 8: SEM of compound 3.

where  $\theta = T - T_s$ ,  $T_s$  is the temperature at the DTG peak. The correlation coefficient  $r$  is computed using the least squares method for equations (1), (2), (3) and (4). Linear curves were drawn for different values of  $n$  ranging from 0 to 2. The value of  $n$ , which gave the best fit, was chosen as the order parameter for the decomposition stage of interest. The kinetic parameters were calculated from the plots of the left hand side of equations (1),(2), against  $1/T$  and against  $\theta$  for equations (3) and (4) (Figure 5, 6). The kinetic parameters for compounds 1, 4 and 5 were calculated for the first step according to the above two methods and are cited in Table 3, 4. The thermodynamic parameters  $\Delta S^\ddagger$ ,  $\Delta H^\ddagger$  and  $\Delta G^\ddagger$  for the three complexes 1, 4 and 5 were computed using the following equations:

$$\Delta S^\ddagger = R [ \ln Zh / kTs ] \quad (5)$$

$$\Delta H^\ddagger = \Delta E^\ddagger - RT_s \quad (6)$$

$$\Delta G^\ddagger = \Delta H^\ddagger - T_s \Delta S^\ddagger \quad (7)$$

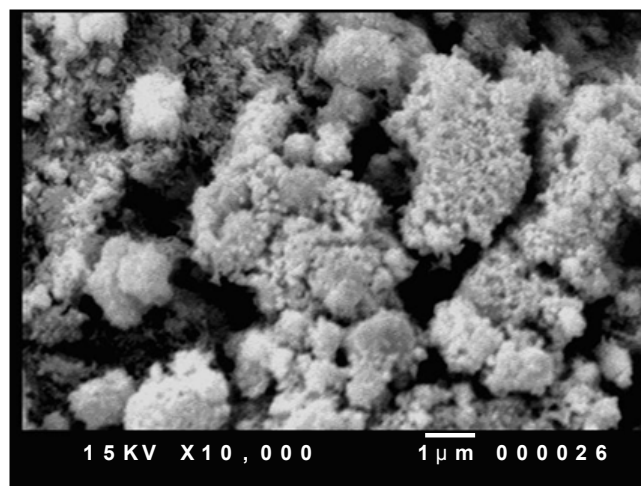


Figure 9: SEM of compound 4.

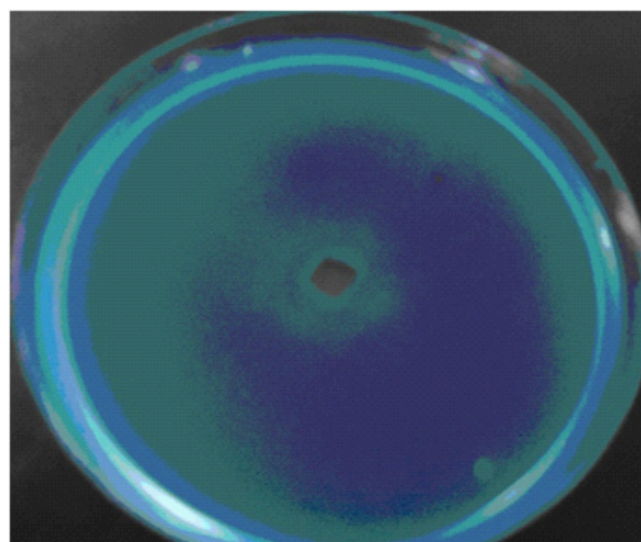


Figure 10: Microbiological screening of compound 1 against *Pseudomonas aeruginosa* (-ve)

where  $h$ , Planck's constant,  $k$ , Boltzmann constant,  $R$ , gas constant and  $T_s$ , temperature at the DTG peak. Negative  $\Delta S^\ddagger$  value for the different stages of decomposition of the complexes suggest that the activated complex is more ordered than the reactants and that the reactions are slower than normal [26-28]. The more ordered nature may be due to the polarization of bonds in the activated state, which might happen through charge transfer electronic transition [29]. The different values of  $\Delta H^\ddagger$  and  $\Delta G^\ddagger$  of the complexes refer to the effect of the structure of the metal ions on the thermal stability of the complexes [30]. The positive values of  $\Delta G^\ddagger$  indicate that the decomposition reaction is not spontaneous.

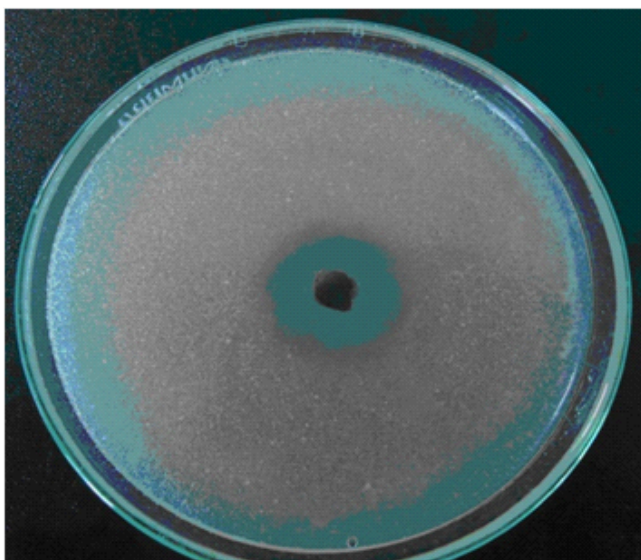


Figure 11: Microbiological screening of compound 4 against *Candida albicans*.

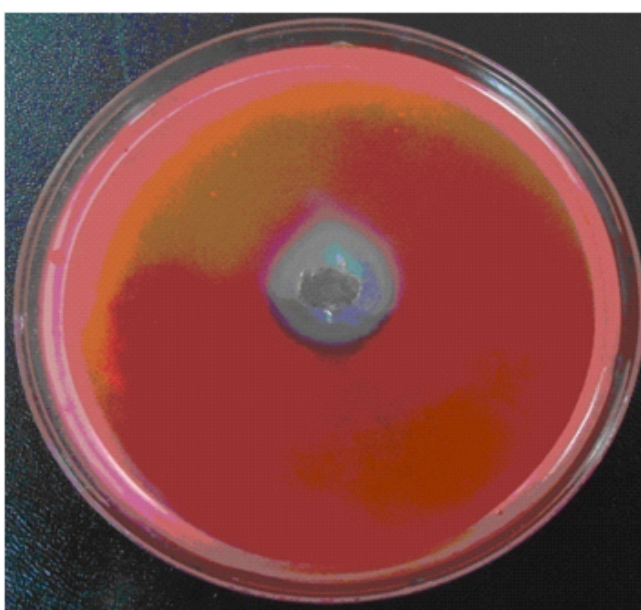


Figure 12: Microbiological screening of compound 5 against *Serratia marcescens*(-ve)

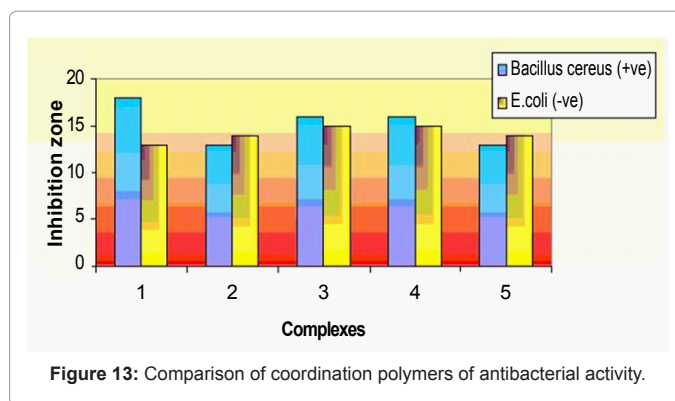


Figure 13: Comparison of coordination polymers of antibacterial activity.

Compound	Step	TG/DTG			Mass Loss(%)
		Ti	Tm	Tf	
1	1st	50	68	156	5.37
	2nd	157	217	244	2.93
	3rd	245	325	371	19.69
	4th	372	475	750	44.07
4	1st	53	64	92	11.01
	2nd	93	131	176	4.31
	3rd	177	201	235	26.30
	4th	236	525	750	32.62
5	1st	150	210	230	1.42
	2nd	231	312	463	33.97
	3rd	464	560	750	18.38

Ti=Initial temperature, Tm=Maximum temperature, Tf=Final temperature.

Table 2: Thermal decomposition data of the compounds in dynamic air.

### X-ray powder diffraction of the complexes

The X-ray powder diffraction patterns were recorded for the coordination polymers 3 and 4. The diffraction patterns indicate that the compounds are crystalline. The crystal lattice parameters were computed with the aid of the computer program TREOR. The crystal data for 3 and 4 metal mixed-ligand compounds belong to the crystal system triclinic (Table 5). The significant broadening of the diffraction patterns suggests that the particles are of nanometer dimensions. XRD of compound 3 is depicted in Figure 7. Scherrer's equation (8) was applied to estimate the particle size of the coordination polymers:

$$D = K\lambda / \beta \cos\theta \quad (8)$$

where  $K$  is the shape factor,  $\lambda$  is the X-ray wavelength typically 1.54 Å,  $\beta$  is the line broadening at half the maximum intensity in radians and  $\theta$  is Bragg angle,  $D$  is the mean size of the ordered (crystalline) domains, which may be smaller or equal to the grain size. The crystal data together with the particle size are recorded in

**Scanning electron micrographs (SEM):** The scanning electron micrographs of copper (II) and cadmium (II) mixed ligand coordination polymers as representatives are given in Figure 8,9. The figures show the different morphologies of the compounds. The rod shape is apparent in the micrograph of compound 3.

### Biological activity

In testing the antibacterial and antifungal activity of these compounds we used more than one test organism to increase the chance of detecting antibiotic principles in tested materials. The data showed that in some cases the ligand has a higher or similar antimicrobial and antifungal activity than the selected standards (chloramphenicol and clotrimazole). Also, the complexes of certain metal ions enhanced the

Compound	Step	Coats-Redfern equation				Horowitz-Metzger equation			
		r	n	E	Z	r	n	E	Z
1	1 <sup>st</sup>	0.9919	0.00	97.1	1.95 x 10 <sup>3</sup>	0.9983	0.00	105.1	5.19 x 10 <sup>4</sup>
		0.9907	0.33	106.2	2.13 x 10 <sup>3</sup>	0.9987	0.33	114.1	1.07 x 10 <sup>5</sup>
		0.9912	0.50	111.2	2.24 x 10 <sup>3</sup>	0.9988	0.50	118.6	1.57 x 10 <sup>5</sup>
		0.9901	0.66	116.0	2.34 x 10 <sup>3</sup>	0.9990	0.66	123.5	2.32 x 10 <sup>5</sup>
		0.9895	1.00	125.7	2.53 x 10 <sup>3</sup>	0.9992	1.00	133.4	5.11 x 10 <sup>5</sup>
		0.9967	2.00	159.7	3.24 x 10 <sup>3</sup>	0.9997	2.00	166.7	6.39 x 10 <sup>6</sup>
4	1 <sup>st</sup>	0.9968	0.00	18.4	5.34 x 10 <sup>6</sup>	0.9996	0.00	29.6	1.57 x 10 <sup>5</sup>
		0.9954	0.33	23.3	4.71 x 10 <sup>2</sup>	0.9998	0.33	34.9	2.42 x 10 <sup>5</sup>
		0.9952	0.50	25.5	5.16 x 10 <sup>2</sup>	0.9999	0.50	37.8	7.07 x 10 <sup>5</sup>
		0.9958	0.66	28.2	5.70 x 10 <sup>2</sup>	0.9999	0.66	40.7	8.05 x 10 <sup>5</sup>
		0.9974	1.00	34.5	6.97 x 10 <sup>2</sup>	1.0000	1.00	47.1	2.25 x 10 <sup>6</sup>
		0.9920	2.00	55.1	11.07 x 10 <sup>2</sup>	1.0000	2.00	69.8	11.53 x 10 <sup>6</sup>
5	1 <sup>st</sup>	0.9972	0.00	51.35	1.03 x 10 <sup>3</sup>	0.9992	0.00	53.06	3.32 x 10 <sup>6</sup>
		0.9984	0.33	63.23	1.27 x 10 <sup>3</sup>	0.9996	0.33	64.15	6.65 x 10 <sup>6</sup>
		0.9991	0.50	70.84	1.42 x 10 <sup>3</sup>	0.9998	0.50	70.75	7.04 x 10 <sup>6</sup>
		0.9994	0.66	77.97	1.56 x 10 <sup>3</sup>	0.9824	0.66	89.34	5.87 x 10 <sup>6</sup>
		0.9999	1.00	95.00	1.80 x 10 <sup>3</sup>	0.9998	1.00	94.13	8.83 x 10 <sup>6</sup>
		0.9997	2.00	156.90	3.09 x 10 <sup>3</sup>	0.9995	2.00	147.50	3.78 x 10 <sup>4</sup>

E in kJ mol<sup>-1</sup>, underlined r in all tables represents the best fit values of n and E

Table 3: Kinetic parameters for the thermal decomposition of the compounds.

Compound	Step	ΔS*	ΔH*	ΔG*
1	1 <sup>st</sup>	-189.44	90.97	139.68
4	1 <sup>st</sup>	-199.43	18.36	118.24
5	1 <sup>st</sup>	-193.06	46.34	116.24

ΔH\*, ΔG\* are in kJ mol<sup>-1</sup> and ΔS\* in kJ mol<sup>-1</sup> K<sup>-1</sup>

Table 4: Thermodynamic parameters for the thermal decomposition of the compounds.

Parameters	3	4
Empirical formula	C <sub>14</sub> H <sub>19</sub> CuN <sub>5</sub> O <sub>6</sub> SCI	C <sub>14</sub> H <sub>19</sub> CdN <sub>5</sub> O <sub>6</sub> SCI
Formula weight	484.45	533.31
Crystal system	triclinic	triclinic
a (Å)	4.153	2.746
b (Å)	10.445	8.002
c (Å)	22.448	11.451
α (°)	66.291	60.601
β (°)	64.065	100.556
γ (°)	77.534	99.210
Volume of unit cell(Å <sup>3</sup> )	800.99	214.83
Particle size(nm)	17	28

Table 5: X-ray diffraction crystal data of the compounds and their particle size.

Compound	B. cereus (G+ve)	S. aureus (G+ve)	S. Marcscens (G-ve)	E. coli (G-ve)	P. aeruginosa (G-ve)	A. flavus	C. albicans	F. oxysporm	T. rubrum	G. candidum	S. brevicaulis
1	18	14	12	13	14	0	0	0	20	17	0
2	13	15	14	14	12	0	0	12	13	16	0
3	16	16	14	15	12	0	12	12	0	18	8
4	16	13	12	15	13	28	15	12	28	14	16
5	13	14	16	14	12	22	0	12	13	14	15

Table 6: Microbiological screening of the compounds.

antimicrobial activity and in some case a higher or similar activity than the selected standards were shown Table 6. Figure 10-13 show the antimicrobial effect for these compounds.

#### Acknowledgement

One of the authors (A. A. M. ALY ) is very grateful to Alexander Von Humboldt Foundation for donating the magnetic susceptibility balance ( MSB-Auto ).

#### References

- Brammer L (2004) Developments in inorganic crystal engineering. Chem Soc Rev 33: 476-489.
- Batten SR, Murray KS (2003) Coordination polymers: design, analysis and application. Coord. Chem Rev 246: 103.
- Yaghi OM, Keeffe MO, Ockwig NW, Chae HK (2003) Reticular synthesis and the design of new materials. Nature 423: 705-714.
- Zou RQ, Sakurai H, Xu Q (2006) Preparation, Adsorption Properties, and Catalytic Activity of 3D Porous Metal–Organic Frameworks Composed of Cubic Building Blocks and Alkali-Metal Ions. Angew Chem Int Ed 45: 2542-2546.
- Carlucci L, Ciani G, Proserpio DM (2003) Polycatenation, polythreading and polyknotting in coordination network chemistry. Coord Chem Rev 246: 247-289.

6. Zhang ZH, Tian YL, Guo YM (2007) Porous Co(II) and Ni(II) coordination polymers based on 5-(4-pyridyl)-1,3,4-oxadiazole-2-thiol for various solvent inclusion. *Inorganica Chim Acta* 360: 2783-2788
7. Oae S (1992) *Organic Sulfur Chemistry: Structure and Mechanism*. CRC Press Boca Raton FL.
8. Singh NK, Bharty MK, Butcher RJ (2009) Synthesis and X-ray crystallographic studies of Ni (II) and Cu (II) complexes of [5-(4-pyridyl)-1,3,4] oxadiazole-2-thione/thiol formed by transformation of N-(pyridine-4-carbonyl)-hydrazine carbodithioate in the presence of ethylenediamine. *Polyhedron* 28: 2443-2449.
9. Zhang ZH, Li CP, Tang GM, Tian YL, Guo YM (2008) {[Cd2(py)2(chdc)(H2O)](H2O)2}n: A unique bilayer coordination polymer with mixed-connected network topology (Hpyt = 5-(4-pyridyl)-1,3,4-oxadiazole-2-thiol and H2chdc = 1,4-cyclohexanedicarboxylic acid). *Inorg Chem Commun* 11: 326-329.
10. Wang YT, Tang GM (2007) One new nickel coordination polymer with an unsymmetric 5-(4-pyridyl)-1,3,4-oxadiazole-2-thione: Synthesis, structure and characterization. *Inorg Chem Commun* 10: 53-56.
11. Wang YT, Tang GM, Qiang ZW (2007) Radius-dependent assembly of complexes with the rigid unsymmetric ligand 5-(2-pyridyl)-1,3,4-oxadiazole-2-thione: Syntheses, structures and luminescence properties. *Polyhedron* 26: 4542-4550.
12. Banu KS, Mondal S, Guha A, Das S (2011) Synthesis, characterization and luminescence properties of polymeric cadmium(II) complexes with imidazole and its derivatives mediated by thiocyanate and dicyanamide anions. *Polyhedron* 30: 163-168.
- 13a) Podunavac SO, Cvetkovic DM (2007) Antibacterial evaluation of some benzimidazole derivatives and their zinc(II) complexes. *J Serb Chem Soc* 72: 459-466.
- 13b) Borisenko VE, Koll A, Kolmakov EE, Rjasnyi AG (2006) *J Mol Struct* 783: 101-115.
14. Serezkhin VN (2007) *Structural Chemistry of Inorganic Actinide Compounds*. Elsevier
15. Lermontov AS, Lermontova EK, Wang YY (2009) Synthesis, structure and optic properties of 2-methylimidazolium and 2-phenylimidazolium uranyl acetates. *Inorganica Chim Acta* 362: 3751-3755.
16. Kwon-Chung KJ, Bennett JE (1992) *Medical mycology*, Lea & Febiger, Philadelphia.
17. Singh M, Butcher RJ, Singh NK (2008) Syntheses and x-ray structural studies of the novel complexes [Ni(en)2(3-pyt)2] and [Cu(en)2](3-pyt)2 based on 5-(3-pyridyl)-1,3,4-oxadiazole-2-thione. *Polyhedron* 27: 3151-3159.
18. Wang YT, Tang GM, Ma WY, Wan WZ (2007) Synthesis and characterization of two new coordination supramolecular structures from a versatile unsymmetric 5-(4-pyridyl)-1,3,4-oxadiazole-2-thione (Hpot) ligand. *Polyhedron* 26: 782-790.
19. Bravo A, Anaconda J (2001) Metal complexes of the flavonoid quercetin: antibacterial properties. *Transition Met Chem* 26: 20-23.
20. Rakha T (2000) Transition metal chelates derived from potassium nicotinoyldithiocarbamate (KHNDc). *Synthesis and Reactivity in Inorganic and Metal-Organic Chemistry* 30: 205-224.
21. Lever ABP (1986) *Inorganic Electronic Spectroscopy*. (2nd Ed) Elsevier Amsterdam.
22. El-Asmy AA, Mounir M (1988) Electrical conductivity, spectral and magnetic properties of some transition metal complexes derived from dimedone bis(4-phenylthiosemicarbazone). *Transition Metal Chemistry* 13:143-146.
23. Anaconda JR, Toledo C (2001) Synthesis and antibacterial activity of metal complexes of ciprofloxacin. *Transition Metal Chemistry* 26: 228-231.
24. Coats A, Redfern J (1964) *Nature* 20:68.
25. Horowitz H, Metzger G (1963) *Anal Chem* 35:1464.
26. Mohamed GG, Hosny WM, Abd El-Rahim MA (2000) New binary and ternary complexes of fluclaxocillin and amino acids with some transition metal. *Synthesis and Reactivity in Inorganic and Metal-Organic Chemistry* 32: 1501-1519.
27. Beg MA, Qaiser MA (1998) Thermal behaviour of bis(diphenyltrifluoromethylphosphine)dichloroplatinum(II). *Thermochemica Acta* 210: 123-132.
28. Pandey OP, Sengupta SK, Tripathi SC (1985) Thermochemistry of metal xanthato complexes. A review *Thermochemica Acta* 96: 155-167.
29. Yusuff KM, Karthikeyan AR (1992) Thermal decomposition kinetics of mixed ligand complexes of cobaloxime with 1-benzyl-2-phenylbenzimidazole. *Thermochemica Acta* 207: 193-199.
30. Emam ME, Kanawy M, Hafe MH (2001) Study of the thermal decomposition of some new cyanine dispersed dyes. *Journal of Thermal Analysis and Calorimetry* 63: 75-83.